Charge Segregation Depends on Particle Size in Triboelectrically Charged Granular Materials

Keith M. Forward, Daniel J. Lacks,* and R. Mohan Sankaran
Department of Chemical Engineering, Case Western Reserve University, Cleveland, Ohio 44106, USA

(Received 22 October 2008; published 16 January 2009)

Experiments are carried out to examine triboelectric charging in granular systems composed of particles that are chemically identical but differ in size. A methodology is developed so that only particle-particle interactions (but not particle-wall interactions) contribute to the charging. Since all particles are chemically identical, there is no apparent driving force for charge transfer, but charging occurs nonetheless, such that smaller particles tend to charge negatively while larger particles tend to charge positively. For bimodal systems, a model for the frequency of collisions of particles with different size predicts the concentrations for which the observed charge segregation is maximized.

DOI: 10.1103/PhysRevLett.102.028001 PACS numbers: 45.70.Mg, 41.20.Cv

An interesting yet poorly understood phenomenon is the electrostatic charging of flowing granular systems with chemically identical particles. It is counterintuitive that charging occurs at all, since charge transfer would seem to be driven by differences in chemical properties. Also, the charging appears to depend on the nature of the particle size distribution (as discussed below), which is surprising because the particles are macroscopic (10–1000 μm) and thus their sizes would seem to be irrelevant in regard to charge transfer. Nevertheless, this charging occurs in a wide range of contexts, including industrial applications such as fluidized beds [1] and pneumatic conveying [2], and natural phenomena such as sand storms [3], dust devils [4,5] and volcanic plumes [6]. One consequence of the charging is that it significantly alters the particle flows [7–9].

In granular systems with chemically identical particles, electrostatic charging occurs with some particles charging negatively and others charging positively. Previous work suggests that a particle size dependence exists for the resulting charge polarity. Field studies on dust devils show that large dipolar electric fields exist, and orient themselves such that the negative pole is at higher altitude and the positive pole is near the ground [10–14]. To explain this result, it has been hypothesized that small particles charge negatively, and since they are lighter, are blown to higher altitudes [8–17]. A similar hypothesis of small particles charging negatively and rising to higher altitudes has been proposed to explain the electric fields that develop in volcanic plumes [18]. In addition, a number of laboratory experiments concluded that small particles charge negatively and large particles charge positively [19–23]. However, these laboratory studies did not limit the cause of charging to only particle-particle interactions (i.e. the particles also interacted with container surfaces made of different materials), or investigate the effects of relative concentration of the various particle sizes. As we described previously, a driving force for particle-size-dependent charge segregation may result from the nonequilibrium dynamics of electrons coupled with particle size differences [24–26].

In this Letter, we investigate the effect of the particle size distribution (PSD) on the electrostatic charging of granular systems with chemically identical particles. Our techniques address the charging due only to particle-particle interactions, so that these effects are decoupled from the effects arising from interactions with other material surfaces.

We focus our investigation on three monodisperse samples of clear soda lime glass (Jaygo, Inc.) with mean particle diameters (standard deviations) of $D = 78\ \mu$m ($\sigma = 13\ \mu$m), $D = 137\ \mu$m ($\sigma = 22\ \mu$m) and $D = 321\ \mu$m ($\sigma = 22\ \mu$m). These monodisperse samples are obtained by sieving a polydisperse sample of soda lime glass, which ensures that all particles are chemically identical. Samples with a bimodal size distribution, hereafter referred to by the smaller particle diameter (D_S) and the larger particle diameter (D_L), are prepared by mixing two monodisperse samples at different mass fractions, w_L ($w_L = m_L/(m_L + m_S)$, where m_L and m_S are the masses of the monodisperse samples of large diameter particles and small diameter particles, respectively).

We have recently developed a methodology to study triboelectric charging resulting only from particle-particle interactions [27,28]. The granular material (approximately 350 mL) is placed on a distribution plate with a single hole at the center. Gas (dry nitrogen) flow through the hole fluidizes only a localized region of the bed (i.e., this granular material) near the bed center. This leads to fountainlike flow, as shown in Fig. 1, in which the particles involved in the flow contact only other particles and no other surfaces (such as the container wall). This particle flow apparatus is operated in a controlled environment (70 Torr nitrogen atmosphere) to reduce contaminants and enhance reproducibility. The particle flow is operated for approximately 120 min (the charging appears to become time independent after about 10 min [27]); all particles remain in the bed after the flow stops. After the particles are charged, the particle flow apparatus is re-

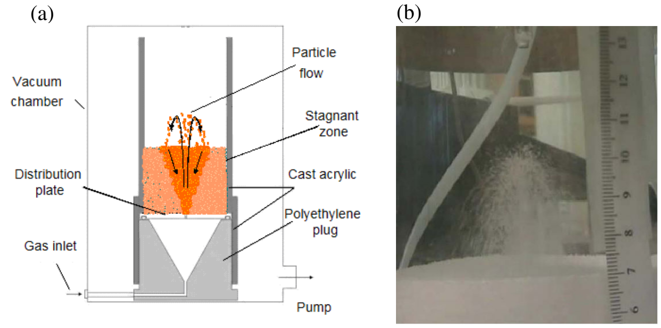

FIG. 1 (color online). (a) Schematic of the particle flow apparatus. Note that due to the single-hole distribution plate, the particle bed differentiates into a zone with flow and a stagnant zone, shown here with different colors. (b) Image of the fountainlike flow that arises from a single-hole distribution plate.

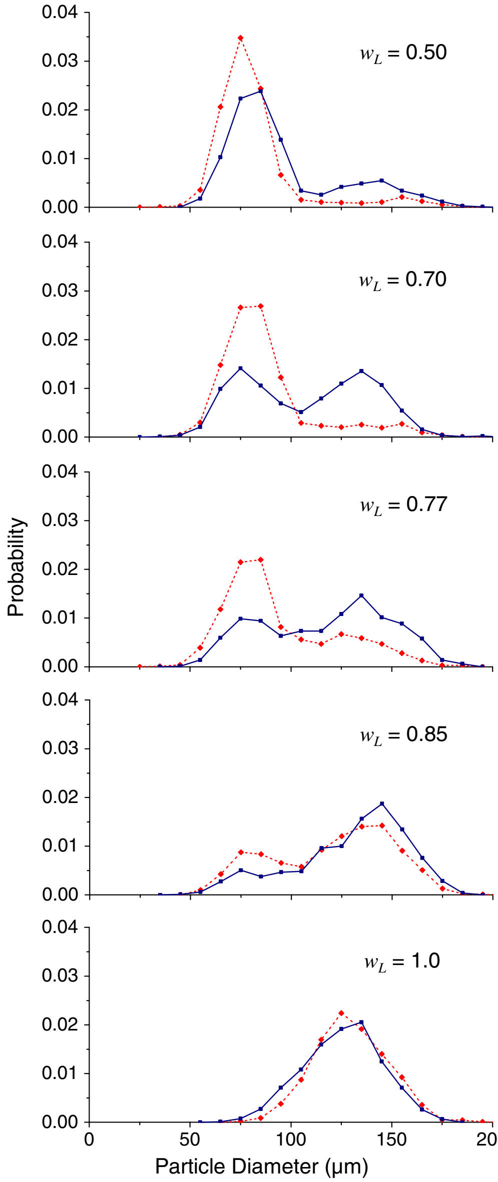

FIG. 2 (color online). Particle size distribution of negatively (dashed line) and positively charged (solid line) particles, for $D_L/D_S = 1.9$ at various mass fractions (w_L) of large particles.

moved from the vacuum chamber and a noncontact method is used to collect particles with specified charge polarity. A 2.5 cm diameter copper disk covered with a 200 μm film of parafilm is suspended ~1 mm above the bed. The disk is held at a positive or negative voltage (10 kV) to extract negatively or positively charged particles, respectively, from the bed. The disk is smaller than the diameter of the flowing region of the bed (~8 cm), and is positioned above only this region, to ensure that only particles involved in the flow are collected. Particles are collected on the parafilm surface, which acts as a spacer so particles do not discharge through the copper disk and fall back to the bed; the particles thus remain attached to the disk as long as the voltage on the disk is maintained. For each polarity, the charging and collection process is performed 3 times, and a total of 0.5–1.2 g of particles (~5000–10 000 particles) are collected with each polarity. After the particles are collected, digital pictures of the positive and negative particle samples are taken through an optical microscope, and the PSDs of each sample are determined (for >1000 particles) by measuring the particle diameters in the images. In addition, the collected particles of each polarity are separated by size with a sieve and the mass of each size cut is obtained.

Figure 2 presents PSDs for the positive and negative particle samples obtained after charging mixtures with various mass fractions of $D_S = 78$ μm and $D_L = 137$ μm particles. For $w_L = 1$, it is seen that the large particles charge both negatively and positively. As w_L decreases, charge segregation becomes apparent, and for $w_L = 0.77$, it is clear that the large particles tend to charge positively and the small particles tend to charge negatively. At $w_L = 0.5$, the results are similar to a monodisperse sample of small particles, where the small particles charge *both* negatively and positively.

These results suggest that charge segregation depends on the relative proportion of the two particle sizes, which can be understood in terms of the probability for collisions between the two types of particles. In a time interval Δt, a particle with diameter D_i moving at velocity v "sweeps out" a volume $\frac{1}{4}\pi(D_i + D_j)^2 v\Delta t$ with respect to a possible collision with a particle with diameter D_j. The probability of a collision between particles of diameters D_i and D_j, $p(D_i, D_j)$, is proportional to the product of this swept out volume and the number densities of particles, with a factor of $\frac{1}{2}$ in the case $i = j$ to eliminate double-counting of collisions. The number density of particles with diameter D_i is given by Nx_i, where N is the total number density and x_i is the number fraction of particles with diameter D_i. Therefore, $p(D_i, D_j) = \zeta_{ij}(Nx_i)(Nx_j)\frac{1}{4}\pi(D_i + D_j)^2 v\Delta t$ where $\zeta_{ij} = \frac{1}{2}$ for $i = j$ and $\zeta_{ij} = 1$ for $i \neq j$. The fraction of collisions occurring between a large particle and a small particle, $f_{L,S}$, is given as $f_{L,S} = p(D_L, D_S)/[p(D_S, D_S) + p(D_L, D_L) + p(D_L, D_S)]$, or

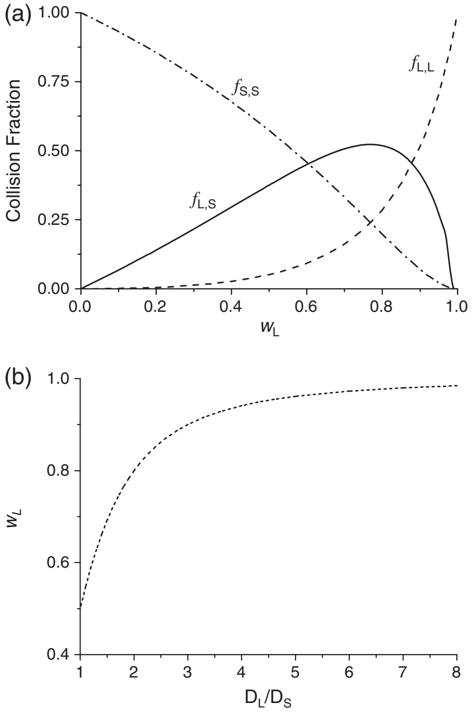

FIG. 3. (a) Collision fractions (see text for definitions) as a function of w_L, for $D_L/D_S = 1.9$. (b) Mass fractions that maximize $f_{L,S}$, for a given D_L/D_S.

$$f_{L,S} = \frac{2(\frac{1+D_L/D_S}{2})^2 x_S x_L}{x_S^2 + (D_L/D_S)^2 x_L^2 + 2(\frac{1+D_L/D_S}{2})^2 x_S x_L}. \qquad (1)$$

The number fractions are calculated from the mass fractions based upon the assumption that the particles are perfect solid spheres,

$$x_L = \frac{w_L}{w_L + w_S(D_L/D_S)^3}, \quad x_S = \frac{w_S(D_L/D_S)^3}{w_L + w_S(D_L/D_S)^3}. \qquad (2)$$

Figure 3(a) shows the calculate collision frequencies as a function of w_L for a sample with $D_S = 78\ \mu$m and $D_L = 137\ \mu$m. Collisions between a small and a large particle will be most prevalent at $w_L = 0.78$ [see Fig. 3(a)], explaining why the most pronounced charge segregation in Fig. 2 is observed for the experiments with $w_L = 0.77$. Figure 3(b) shows the values of w_L that maximize $f_{L,S}$ as a function of D_L/D_S; the propensity for charge segregation is predicted to be the greatest at these concentrations.

Table I gives the results for all experiments carried out [the mass fractions examined should be considered in comparison to Fig. 3(b)]. The number fractions of large particles in the negatively charged sample,x_L^-, and in the positively charged sample,x_L^+, are obtained by two independent methods. The count-based number fraction is obtained from the optical microscope images, and the mass-based number fraction is obtained from masses of the sieved samples; the two methods give consistent results. To quantify the extent of charge segregation, we define the charge segregation factor, ξ,

$$\xi = \sqrt{\frac{x_L^+}{x_L^-}\frac{x_S^-}{x_S^+}}. \qquad (3)$$

The charge segregation factor represents the geometric mean of the deviations from overall neutrality for the small and large particles. In all experimental trials, large particles tend to charge positively and small particles tend to charge negatively, as indicated by values of $\xi > 1$. Note that for each bimodal system the most pronounced charge segregation occurs near the mass fractions predicted in Fig. 3(b).

Figure 4 compares the results for the three bimodal samples, each at the mass fraction that maximizes charge segregation [i.e., the value of w_L that maximizes $f_{L,S}$, as shown in Fig. 3(b)]. As D_L/D_S increases, the charge segregation is enhanced, as evident in Fig. 4 and Table I ($\xi = 1.7$, 3.8 and 4.3 for $D_L/D_S = 1.8$, 2.3 and 4.3, respectively). Figure 4 also shows that charge segregation depends on the relative size difference between particles, and *not* on the absolute particle sizes—e.g., the $D = 137\ \mu$m sample tends to charge positively when mixed with the $D = 78\ \mu$m sample, but tends to charge negatively when mixed with the $D = 321\ \mu$m sample.

TABLE I. Results for the charge segregation in soda lime glass bimodal samples. The error estimate for the charge segregation factor is determined from the difference in results obtained using the mass-based and count-based number fractions.

	w_L	x_L^-		x_L^+		ξ
		By mass	By count	By mass	By count	
$D_L/D_S = 1.9$	0.50	0.19	0.08	0.23	0.25	1.4 ± 0.5
	0.70	0.29	0.13	0.43	0.49	1.8 ± 0.7
	0.77	0.44	0.27	0.61	0.60	1.7 ± 0.5
	0.85	0.61	0.65	0.70	0.78	1.3 ± 0.2
$D_L/D_S = 2.3$	0.70	0.08	0.05	0.35	0.39	3.3 ± 0.4
	0.85	0.14	0.20	0.66	0.83	3.8 ± 1.5
	0.93	0.15	0.29	0.65	0.74	2.9 ± 1.1
$D_L/D_S = 4.3$	0.85	0.09	0.08	0.14	0.20	1.5 ± 0.3
	0.93	0.17	0.09	0.77	0.71	4.4 ± 1.4
	0.99	0.81	0.88	>0.92	0.93	1.5 ± 0.4

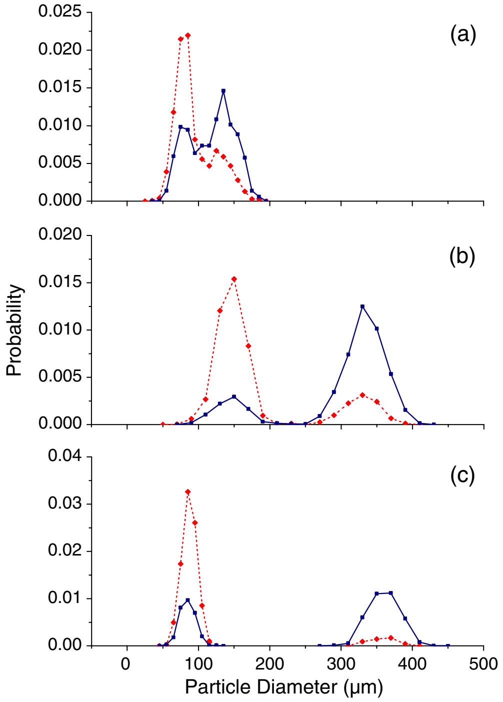

FIG. 4 (color online). Particle size distribution of negatively (dashed line) and positively charged (solid line) particles as a function of D_L/D_S at the mass fractions where charge segregation is most pronounced (see text). (a) $D_L/D_S = 1.9$, $w_L = 0.77$. (b) $D_L/D_S = 2.3$, $w_L = 0.85$. (c) $D_L/D_S = 4.3$, $w_L = 0.93$.

In addition to the soda lime glass samples, we studied the charging behavior of a polyethylene resin (Dow Chemical Company). Monodisperse samples of particles with $D = 605\ \mu\text{m}$ ($\sigma = 99\ \mu\text{m}$) and $D = 300\ \mu\text{m}$ ($\sigma = 62\ \mu\text{m}$) are obtained by sieving a polydisperse sample. Figure 5 shows results for the PSDs obtained for a mixture with $w_L = 0.80$. The results confirm that for polyethylene, as for soda lime glass, large particles tend to charge positively and small particles tend to charge negatively.

A key factor for the validity of our methodology is that identical PSDs are probed in the particle extraction process for the positive and negative particles. Since there is no sampling bias between the positive and negative samples, our conclusion in regard to the size dependence of the particle polarity is valid even if the particles sampled in the particle extraction process do not match the overall concentration of the bed. We note that the particle extraction process does not, in fact, sample the particles in the mixture uniformly—this is evident in the results in Table I, which show that the w_L's for the positive and negative samples are both smaller than the w_L for the overall mixture. This occurs because the particle extraction process preferentially collects smaller particles as these particles are more easily pulled against gravity from the bed to the disk. While the fluidization process could cause nonideal mixing of small and large particles (size segregation), our tests of the size distribution at the top of the bed after flow (obtained by scooping a layer) indicate that these effects are not significant. As stated above, since there is no sampling bias between the positive and negative samples, the conclusion that small particles tend to charge negatively and large particles tend to charge positively is unambiguous.

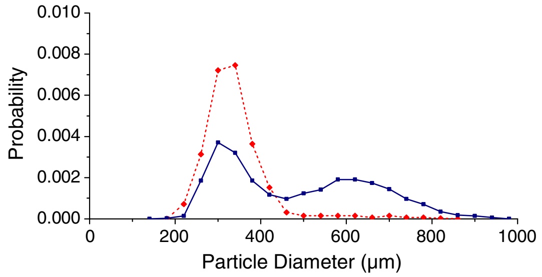

FIG. 5 (color online). Particle size distribution of negatively (dashed line) and positively charged (solid line) polyethylene resin particles. The sample contained particles with $D_L = 605\ \mu\text{m}$ and $D_S = 300\ \mu\text{m}$, at $w_L = 0.8$.

This project was funded by the Dow Chemical Company.

---

*daniel.lacks@case.edu

[1] G. Hendrickson, Chem. Eng. Sci. **61**, 1041 (2006).
[2] S.-C. Liang *et al.*, Ind. Eng. Chem. Res. **35**, 2748 (1996).
[3] C. D. Stow, Weather **24**, 134 (1969).
[4] H. F. Eden and B. Vonnegut, Science **180**, 962 (1973).
[5] A. A. Mills, Nature (London) **268**, 614 (1977).
[6] J. S. Gilbert *et al.*, Nature (London) **349**, 598 (1991).
[7] M. F. Al-Adel *et al.*, Ind. Eng. Chem. Res. **41**, 6224 (2002).
[8] J. F. Kok and N. O. Renno, Phys. Rev. Lett. **100**, 014501 (2008).
[9] T. Shinbrot and H. J. Herrmann, Nature (London) **451**, 773 (2008).
[10] G. D. Freier, J. Geophys. Res. **65**, 3504 (1960).
[11] W. D. Crozier, J. Geophys. Res. **69**, 5427 (1964).
[12] C. D. Stow, Rep. Prog. Phys. **32**, 1 (1969).
[13] A. I. I. Ette, J. Atmos. Terr. Phys. **33**, 295 (1971).
[14] W. M. Farrell *et al.*, J. Geophys. Res. **109**, E03 004 (2004).
[15] O. Melnik and M. Parrot, J. Geophys. Res. **103**, 29 107 (1998).
[16] S. J. Desch and J. N. Cuzzi, Icarus **143**, 87 (2000).
[17] W. M. Farrell *et al.*, J. Geophys. Res. **111**, E01 006 (2006).
[18] T. Miura *et al.*, Bull. Volcanol. **64**, 75 (2002).
[19] P. Cartwright *et al.*, IEEE Trans. Ind. Applicat. IA- **21**, 541 (1985).
[20] F. S. Ali *et al.*, J. Electrost. **45**, 139 (1998).
[21] H. Zhao *et al.*, J. Electrost. **55**, 261 (2002).
[22] H. Zhao *et al.*, IEEE Trans. Ind. Appl. **39**, 612 (2003).
[23] I. I. Inculet *et al.*, Chem. Eng. Sci. **61**, 2249 (2006).
[24] D. J. Lacks and A. Levandovsky, J. Electrost. **65**, 107 (2007).
[25] N. Duff and D. J. Lacks, J. Electrost. **66**, 51 (2008).
[26] D. J. Lacks *et al.*, Phys. Rev. Lett. **100**, 188305 (2008).
[27] K. M. Forward *et al.*, Ind. Eng. Chem. Res. (to be published).
[28] K. M. Forward *et al.*, J. Electrost. (to be published).